A graphene oxide center dot streptavidin complex for biorecognition - towards affinity purification

Liu, Z.; Jiang, L.; Galli, F.; Nederlof, I.; Olsthoorn, R.R.C.L.; Lamers, G.E.M.; ... ; Abrahams, J.P.

A Graphene Oxide·Streptavidin Complex for Biorecognition – Towards Affinity Purification

By *Zunfeng Liu,* Linhua Jiang, Federica Galli, Igor Nederlof, René C. L. Olsthoorn, Gerda E. M. Lamers, Tjerk. H. Oosterkamp,* and *Jan Pieter Abrahams**

In our postgenomic era, understanding of protein-protein interactions by characterizing the structure of the corresponding protein complex is becoming increasingly important. An important problem is that many protein complexes are only stable for a few minutes. Dissociation will occur when using the typical, time-consuming purification methods such as tandem affinity purification and multiple chromatographic separations. Therefore, there is an urgent need for a quick and efficient protein-complex purification method for 3D structure characterization. The graphene oxide (GO)·streptavidin complex is prepared via a GO·biotin·streptavidin strategy and used for affinity purification. The complex shows a strong biotin recognition capability and an excellent loading capacity. Capturing biotinylated DNA, fluorophores and Au nanoparticles on the GO·streptavidin complexes demonstrates the usefulness of the GO·streptavidin complex as a docking matrix for affinity purification. GO shows a high transparency towards electron beams, making it specifically well suited for direct imaging by electron microscopy. The captured protein complex can be separated via a filtration process or even via on-grid purification and used directly for single-particle analysis via cryo-electron microscopy. Therefore, the purification, sample preparation, and characterization are rolled into one single step.

1. Introduction

The need for an electron-transparent substrate that can specifically capture tagged protein complexes prompted us to fabricate streptavidin-functionalized graphene oxide (GO). Such a template should allow structural studies of biotinylated protein complexes by transmission electron microscopy (TEM) to understand protein-protein interactions. Protein-protein interactions are of central importance for virtually every process in living cells.[1] For example, signals from the exterior of a cell are mediated to the inside of that cell by protein-protein interactions of the signalling molecules. This process, called signal transduction, plays a fundamental role in many biological processes and in many diseases.[2] Therefore, information about these interactions improves our understanding of diseases and can provide the basis for new therapeutic approaches. During this signal transduction, two or more proteins interact with one another to form a protein complex by non-covalent interactions.[3] These complexes form various types of molecular machines that perform a vast array of biological functions.[4] Characterization of these complexes is essential to understand many biological processes.

Different methods have been developed to investigate the structural aspects of protein-protein interactions, including X-ray diffraction (XRD), NMR spectroscopy, cryo-electron microscopy (EM), and, to characterize the complex composition, mass spectroscopy.[1,5] Other methods for characterization include co-immunoprecipitation,[6] and surface plasmon resonance,[7] in which affinity pairs are used to trap complexes. All of the above procedures require purification, concentration and sample preparation, and these steps can in many instances form the major bottleneck in the procedure. Single-particle cryo-EM is a well-known method for studying the low-resolution 3D structures of protein complexes.[5a] Sample preparation for cryo-EM is relatively straightforward, as it does not require a crystallization step (as for XRD) or a particularly large amount of sample (multi mg) at high concentrations (as for NMR spectroscopy).[8]

Protein-complex purification is still a key step for the accurate characterization of the protein complex. Tandem-affinity-purification[9] and multiple-chromatographic-separation steps[10]

[*] Dr. Z. Liu, Dr. L. Jiang, I. Nederlof, Prof. J. P. Abrahams
Department of Biophysical Structural Chemistry
Leiden Institute of Chemistry
Gorlaeus Laboratories
Leiden University
P.O. Box 9502, 2300 RA Leiden (The Netherlands)
E-mail: liuz2@chem.leidenuniv.nl; abrahams@chem.leidenuniv.nl

Dr. F. Galli, Prof. T. H. Oosterkamp
Leiden Institute of Physics, University of Leiden
2333 CA Leiden (The Netherlands)

Dr. R. C. L. Olsthoorn
Leiden Institute of Chemistry, LIC/Molecular Genetics
2300 RA Leiden (The Netherlands)

Dr. G. E. M. Lamers
Institute Biology Leiden
2333 BE Leiden (The Netherlands)

DOI: 10.1002/adfm.201000761

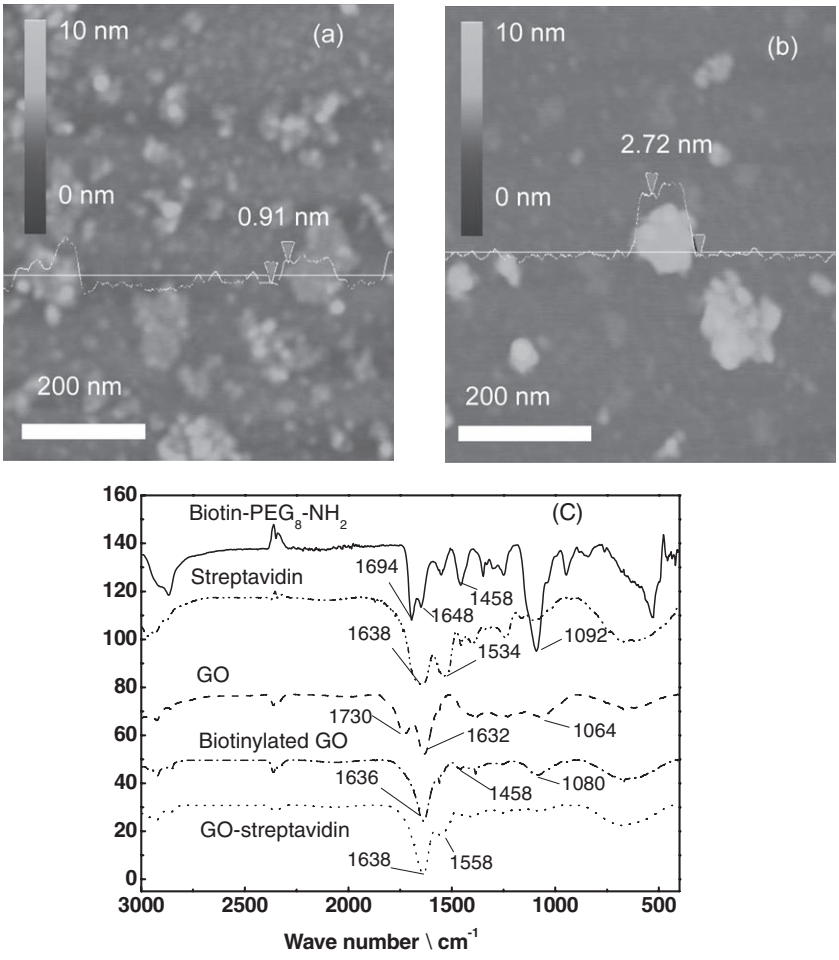

Figure 1. a) Atomic force microscopy (AFM) image of GO. b) AFM image of biotinylated GO. The cross-sectional analysis shows a height of 0.91 nm for the GO and 2.72 nm for the biotinylated GO. c) FTIR spectra of biotin-PEG_8-NH_2, streptavidin, GO, biotinylated GO, and GO·streptavidin in the range of 3000–400 cm^{-1}.

are typical purification methods for stable protein complexes. Protein-protein interactions are usually dynamic processes and the complexes have different degrees of stability over time: many protein complexes with fast kinetics (high K_{on}, high K_{off}) and/or low affinity have a half life of only several or several tens of minutes.[5b] Time-consuming procedures may result in the dissociation of unstable protein complexes during the purification process. Chemical crosslinking methods using crosslinking agents or UV light have been developed to stabilize protein complexes before the purification process.[11] However, such methods are not universally applicable and are always inefficient because there are differences in crosslinking efficiency due to differences in the reactivity, caused by differences in geometry and alignment. Furthermore, artefacts cannot be excluded. These factors may result in inaccuracies in structural determination and a misunderstanding of the protein-protein interaction.[12] Therefore, there is an urgent need to develop a purification method in which the native structure of the protein complex is retained.

Magnetic streptavidin beads efficiently capture biotinylated protein complexes by use of the extraordinarily high affinity constant of the streptavidin-biotin interaction, ~10^{14} dm^3 mol^{-1}.[13] The target protein complex together with the magnetic beads can be quickly separated by the use of a magnet, but cannot be used directly for single-particle analysis via cryo-EM because the magnetic beads strongly interfere with the electron beam.

Graphene, a single layer of carbon atoms in a 2D, close-packed, honeycomb lattice has unique properties, such as exceptional thermal,[14] mechanical,[15] and electrical properties.[16] Due to its low atomic number and two-dimensional nature, graphene has a high electron transparency; its high conductivity can reduce charging effects and improve imaging stability; furthermore, graphene has good flexibility and high stiffness, allowing it to withstand harsh treatment and be mechanically versatile. Therefore, single-layered, 1.6 nm, self-assembled carbon nanosheets[17] and graphene membranes[18] have been used as effective sample-support films for TEM. The oxide form of graphene, graphene oxide, which shows a similar high electron transparency and high stiffness to graphene and has an easy fabrication method, has also been used successfully as a sample support for TEM. It has also been proven to be a promising substrate for nanoparticles (NPs), macromolecules, and biological materials.[19] Furthermore, given its functional –OH and –COOH groups,[20] it also allows the introduction of new functional moieties.

Motivated by these considerations, we synthesized the GO·streptavidin complex, which can be used to capture biotinylated protein complexes via the streptavidin-biotin interaction, as virtually any protein can be biotinylated in vivo in living cells by genetic manipulation, resulting in the addition of a small peptide that is specifically biotinylated by the enzyme BirA.[21] The GO·streptavidin complex together with the target protein complex can be separated from other soluble components via a filtration process or via on-grid separation. Thus, it can directly be used for structural characterization with TEM because of the high transparency of GO to the electron beam. Therefore, such a purification process rolls the purification, sample preparation and characterization into a single step that can be handled quickly enough to retain the native structure of the protein complex.

2. Results and Discussion

The GO was prepared using a modification of Hummers' method:[20] in a highly oxidizing mixture of $KMnO_4$/H_2SO_4/KNO_3, oxygen functionalities such as hydroxyl, epoxyl, carboxyl, and other carbonyl groups were introduced on the edge and in the plane of the graphene sheet,[22] resulting in good

solubility of the GO in many kinds of solvent, including H_2O, dimethylformamide (DMF), *N*-methyl-2-pyrrolidone (NMP), and tetrahydrofuran (THF), for example.[23] After the oxidizing treatment and a sonication that dispersed the GO in DMF, the GO turned out to be fragmented into small pieces that had a size of several tens to hundreds of nanometers and a thickness of ~0.9 nm, as shown in **Figure 1a**. The Fourier transform infrared (FTIR) spectrum of GO in Figure 1c shows the presence of –C=O (ν = 1730 cm^{-1}), aromatic –C=C (ν = 1632 cm^{-1}), and alkoxy –C–O (ν = 1064 cm^{-1}) stretches, as has been reported previously.[24] The –C=O moieties can be ascribed to the –COOH,[22a,25] as well as to other carbonyl-containing groups such as ketones and/or quinones,[22b,26] Elemental analysis of GO showed that the weight percentages of C, H and O were 43.7%, 2.9%, and 53.4%. The thermogravimetric analysis (TGA) of GO in N_2 (Figure S1 in the Supporting Information (SI)) shows a weight loss of 7% below 100 °C, which is accounted for by the weight loss of adsorbed H_2O. The sharp weight loss (28%) at around 200 °C is accounted for by the decomposition of labile oxygen-containing groups, and the following slow and steady weight loss (27%) above 250 °C can be ascribed to desorption of more-stable oxygen functional groups.[27] Omitting the H and O that the physically adsorbed H_2O accounts for, the weight percentages of the C, H and O in GO were 47.0%, 2.3%, and 50.7%, indicating a C:H:O molar ratio of ~1:0.6:0.8, which suggests a high oxidation degree of the graphene compared to that in the literature.[27] This is favourable for biotinylation and the following complexation of GO with streptavidin. The UV-vis spectrum in Figure S2a in the SI indicates that the GO absorbs decreasingly slowly with wavelength, while streptavidin almost does not absorb above 300 nm. Therefore, we measured a calibration curve for determining the concentration of GO by absorbance at 320 nm, as shown in Figure S2b–c in the SI. The curve shows good linearity over a wide concentration range and was used to calculate the concentration of GO.

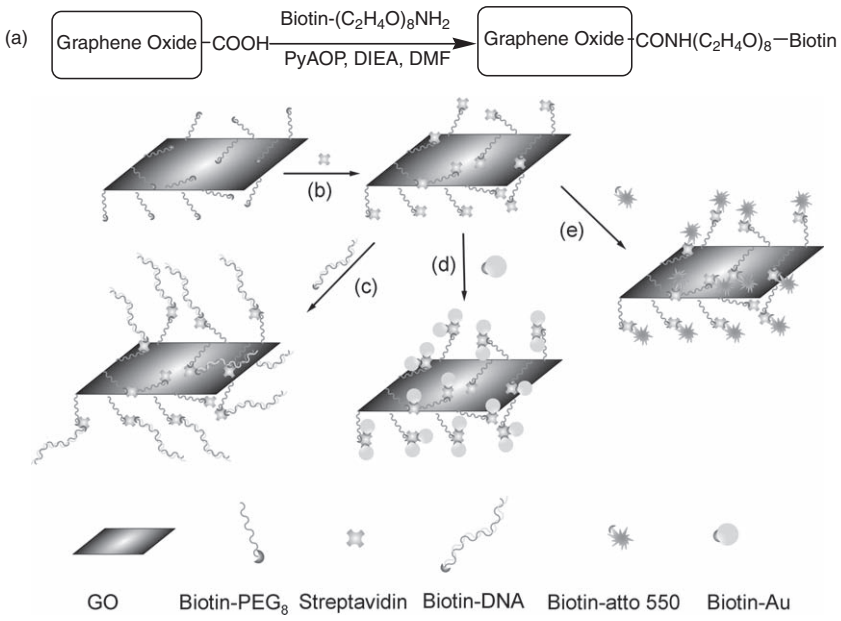

Figure 2. a) Reaction scheme of the biotinylation of GO. b) Schematic representation of the preparation of the GO·streptavidin complex via the biotin-streptavidin interaction. c–e) Schematic representation of preparation of GO·DNA (c), GO·Au NPs (d) and GO·atto 550 (e) complexes using GO·streptavidin as the docking matrix.

Biotin binds to streptavidin in a 4:1 stoichiochemistry.[28] This enables sandwich-binding architectures on GO, that is, [biotinylated GO]·[streptavidin]·[biotinylated species of interest]. We have used a similar strategy to prepare single-walled carbon nanotube (SWCNT)·streptavidin complexes.[29] Biotin has stable chemical properties and tolerates relatively harsh reaction conditions in different solvents, allowing biotinylation of GO through a variety of routes and the introduction of other functional elements such as a poly(ethylene glycol) (PEG) segment to prevent non-specific absorption. Here, GO was biotinylated via the coupling reaction between –NH_2, using an amine-terminated biotin (*O*-(2-aminoethyl)-*O*′-[2-(biotinylamino)ethyl] octaethylene glycol) (biotin-PEG_8–NH_2), and the –COOH of GO, as shown in **Figure 2a**. A short segment of $(C_2H_4O)_8$ was introduced between the GO and biotin in order to render the graphene sheet soluble in H_2O. This segment also served as a spacer, decreasing the steric hindrance between the GO and streptavidin, and also reduced non-specific binding between the GO and the protein. The biotinylated GO indeed was found to be soluble in H_2O without any detergent.

Figure 1b shows a typical biotinylated GO, having a thickness of ~2.7 nm. The thickness was increased after biotinylation, which can be attributed to the biotin-PEG_8, crosslinked to the GO. The FTIR spectrum in Figure 1c confirms the presence of the biotin-PEG_8, with peaks at 1458 cm^{-1} (corresponding to CH_2 bending) and at 1092 cm^{-1} (corresponding to the vibration of the ether group in the PEG segment), which also exist in the FTIR spectrum of GO·biotin (ν = 1458 cm^{-1} and ν = 1080 cm^{-1}).

Biotinylated GO in H_2O can interact with streptavidin to form a GO·streptavidin complex, as shown in Figure 2b. Note that the assembly of biotinylated GO and streptavidin is a crosslinking aggregation system[30] because the functionalities of both the biotinylated GO (>>2) and streptavidin (4) are larger than 2, which is typical for a crosslinking polymerization system.[31] Such a crosslinking aggregation system has been discussed in detail in our previous SWCNT·streptavidin study.[29] Summarizing, crosslinking should be avoided and a high loading of streptavidin on GO is required for the successful generation of single-sheet GO·streptavidin. This can be achieved by mixing biotinylated GO with a vast excess of streptavidin, as shown in **Figure 3a**.

By carefully adding a dilute biotinylated GO solution (0.01 mg mL^{-1}, 10 mL) dropwise into a streptavidin solution (1 mg mL^{-1}, 20 mL) followed by thorough washing, a complex of GO·streptavidin, with the GO covered by streptavidin, was synthesized. The FTIR spectrum of the GO·streptavidin in Figure 1c confirms the presence of streptavidin. The streptavidin shows strong peaks at 1638 cm^{-1} (corresponding to

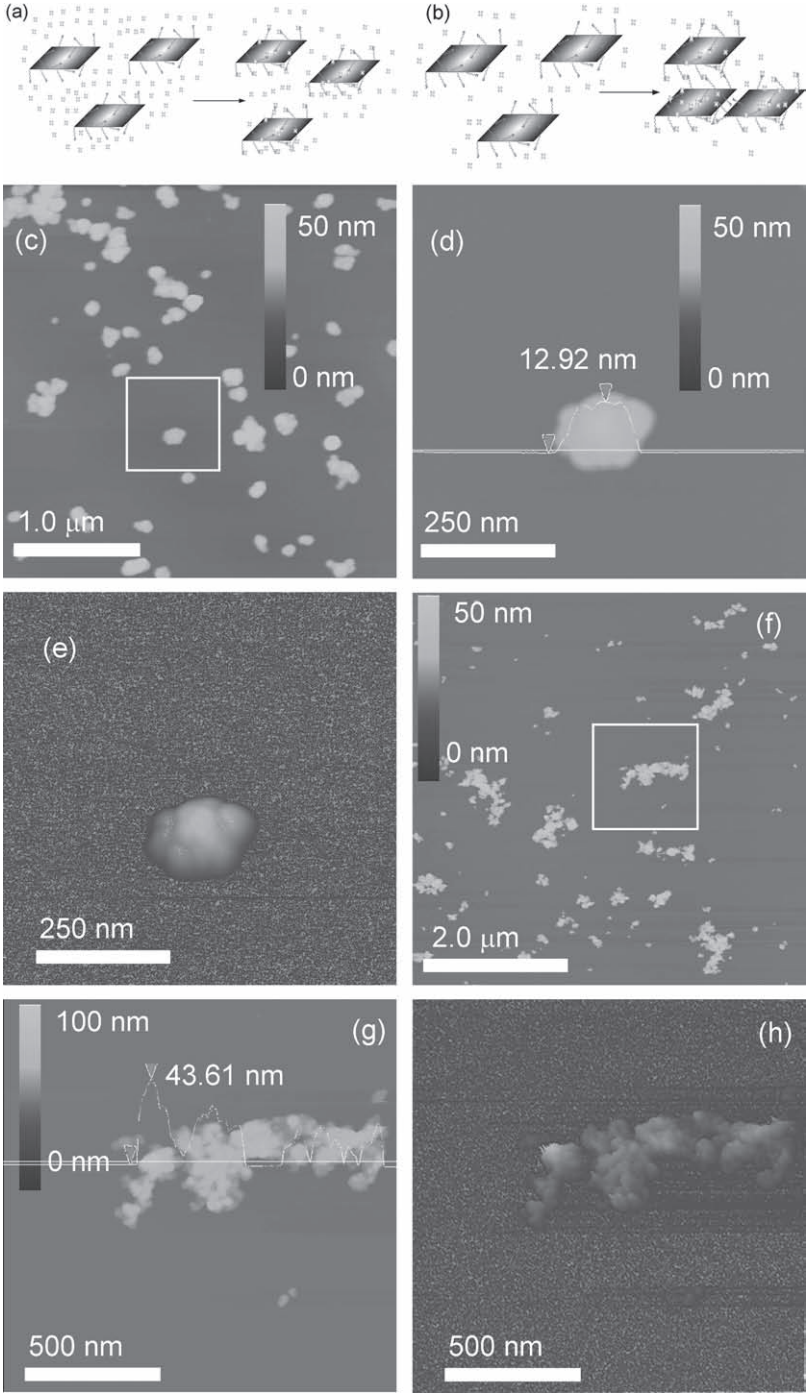

Figure 3. Schematic representation of the crosslinking aggregation system of biotinylated GO with streptavidin in different conditions: a) excess amount of streptavidin compared to biotinylated GO; b) comparable amounts of GO-immobilized biotin and streptavidin. c–e) AFM images of GO·streptavidin prepared with an excess of streptavidin, preventing crosslinking of the GO flakes (biotinylated GO (0.01 mg mL^{-1}, 10 mL); streptavidin (1 mg mL^{-1}, 20 mL)): overall image (c), the zoomed-in image (d), and a 3D-view of 3d is shown in 3e. The cross-sectional analysis indicates the thickness of the GO·streptavidin complex to be ~13 nm. f–h) AFM images of GO·streptavidin prepared with a smaller amount of streptavidin, allowing (limited) crosslinking of the GO flakes (biotinylated GO (0.01 mg mL^{-1}, 10 mL); streptavidin (1 mg mL^{-1}, 10 mL)): the overall image (f), the zoomed-in image (g), and a 3D-view of 3g is shown in 3h. The cross-section analysis indicates that the aggregates of the GO·streptavidin complex could reach ~44 nm at the site of highest thickness.

amide I: the –C=O stretch of the protein) and 1534 cm^{-1} (corresponding to amide II: the –C–N stretch and –C–N–H deformation), which are also present in the FTIR spectrum of GO·streptavidin (ν = 1638 cm^{-1} and ν = 1558 cm^{-1}). Figure 3c shows the AFM images of the GO·streptavidin complexes. The GO was fully covered by streptavidin molecules, as indicated by the cross-sectional analysis in the zoomed-in image (Figure 3d), which shows a complex having a thickness of ~13 nm. The increase in the thickness of the GO·streptavidin complex can be attributed to the attachment of streptavidin molecules to both sides of the GO. Figure 3e shows the 3D view corresponding to Figure 3d, in which the streptavidin molecules can be clearly seen. Decreasing the amount of streptavidin will inevitably increase the possibility of the crosslinking, as shown in Figure 3b. Figure 3f shows the AFM image when only half the amount of streptavidin (10 mg) was used, resulting in large aggregates of up to several micrometers. Figure 3g shows a zoomed-in image of Figure 3f, where the highest position was ~44 nm, judged from the cross-sectional analysis of the aggregate. A 3D-view corresponding to Figure 3g is shown in Figure 3h, demonstrating the irregular 3D aggregation via lateral expansion and longitudinal thickening of the biotinylated GO sheets with streptavidin.

Figure 3c shows that most of the GO·streptavidin complexes exist as separate particles; a few of the GO·streptavidin complexes are connected to one another, forming a branched structure, but almost no 3D crosslinked structures were observed. Note that all of the streptavidin molecules in Figure 3c and 3d are ligated and none occur as tetramers, separated from the GO. This indicates that all of the unligated streptavidin was removed by repeated filtration and that almost no streptavidin molecules dissociated from the GO·streptavidin complex. The surface properties of the GO·streptavidin complex are completely altered compared to undecorated GO, because of the high coverage of the streptavidin on the GO. The GO and the biotinylated GO did not stick to a pure mica surface and could be removed by rinsing with H_2O, but they absorbed tightly on an $–NH_2$-covered mica surface (treated with 3-aminopropyltriethanoxysilane (APTES)).[32] The exact mechanism of the strong absorption of the $–NH_2$-modified surface with GO is unclear. By considering the interaction between its allotrope (carbon nanotubes) and $–NH_2$,[33] the possible mechanism might be the interaction between the free-electron pair of amine groups and the aromatic graphene skeleton.[33,34] In contrast, the GO·streptavidin complex did stick tightly to the untreated mica surface, as shown in Figure S4a in the SI. The

observed absorption of the GO·streptavidin complex onto the mica surface can be attributed to the charge interaction between the mica and the streptavidin moieties;[35] similar absorption on mica was also observed for the SWCNT·streptavidin complex.[29] We found that the GO·streptavidin complex could also stick to the $-NH_2$-treated mica (Figure S4b in the SI), whereas the SWCNT·streptavidin complex could not, possibly due to the different complex structure and carbon-skeleton properties. The SWCNTs have a high mechanical strength, while the GO has a flexible surface with wrinkles in the plane. This might allow incompletely decorated parts of the GO to partially contact the surface and interact with the $-NH_2$ groups.

Using a Bradford assay, the loading of streptavidin on GO was measured. The calibration curve of the Bradford assay experiments is shown in Figure S3 of the SI. In a GO·streptavidin solution containing 42.1 μg mL^{-1} of GO, there were 13.3 μg mL^{-1} of streptavidin, indicating a loading content of 1 mg of streptavidin for every 3.2 mg of GO. By considering that the C content of GO is 43.7%, there was therefore 1 mg of streptavidin every $42.1 \times 43.7\%/13.3 = 1.38$ mg of carbon, indicating that there was 1 streptavidin tetramer per $(1/60\ 000)/(1.38/12) = 6900$ carbon atoms. Because there are 38 C atoms per 1 nm^2 of the graphene sheet,[36] there was 1 streptavidin tetramer every $1/(6900/38) \approx 180$ nm^2 (i.e., a square of 13.4 nm × 13.4 nm) of graphene.

In order to demonstrate that the GO·streptavidin complexes described here can be used to capture biotinylated molecules, we investigated the biotin-binding activity using different biotinylated species such as biotinylated DNA, biotinylated fluorophores, and biotinylated Au NPs, as illustrated in Figure 2c–e.

A biotinylated DNA having 1000 base pairs was used to form GO·DNA conjugates. We investigated these complexes with AFM, which required them to be immobilized on mica. However, because DNA is negatively charged, it does not stick to the mica surface and is easily removed by rinsing with H_2O. Therefore, we prepared a GO·streptavidin-coated mica surface, and then incubated it with a biotinylated DNA solution to prepare the GO·DNA conjugates. This method rolls the synthesis, purification, and AFM imaging of the GO·DNA conjugate into a single step. The same preparation procedure was used for the synthesis of GO·atto 550 and GO·Au NPs conjugates.

Figure 4 shows AFM images of the GO·DNA conjugates prepared from GO·streptavidin and biotin-DNA. Almost all of the GO·streptavidin complexes were linked to many DNA strands (Figure 4a). This indicates a good biotin-binding ability and a high biotin-loading capacity of the GO·streptavidin complex. The zoomed-in image (Figure 4b) suggests that the loading of DNA strands on a single GO was so high that they criss-crossed or compactly stacked onto one another. They were not evenly dispersed around the GO·streptavidin complex, which may have been caused by H_2O rinsing and subsequent N_2-blow-drying. The compact stacking may be due to the extended aggregation, perhaps enhanced by Marangoni effects.[29] The high loading with DNA strands confirms the high coverage of streptavidin of

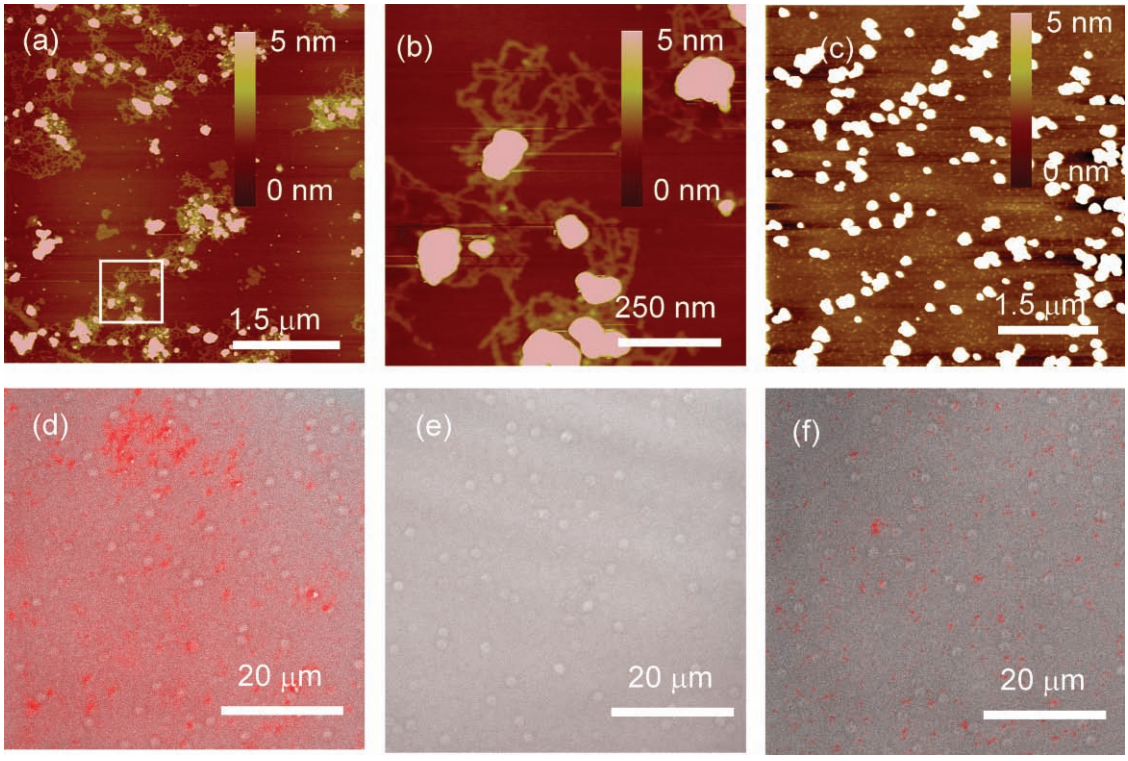

Figure 4. a–c) AFM images of GO·DNA conjugates prepared via the biotin-streptavidin affinity interaction, using: the GO·streptavidin complexes as the docking matrix (a) (the zoomed-in image is shown in Figure 4b), and the GO complexing with non-biotinylated DNA (c). d–f) Fluorescence images: biotinylated atto 550 on GO·streptavidin-coated mica after washing with water (d), atto-550 biotin on mica without GO·streptavidin after rinsing with water (e), and non-biotinylated atto 550 on GO·streptavidin-coated mica after washing with water (f).

the GO. In order to show that the biotin-DNA was linked to the GO via specific streptavidin-biotin recognition, and not by non-specific interactions, we performed a control experiment using DNA *without* a biotin tag. Not a single DNA strand was found that was linked to a GO·streptavidin complex (Figure 4c).

The fluorescence image of conjugates of GO·atto 550, prepared from GO·streptavidin and biotin-atto 550 (a fluorescent dye), is shown in Figure 4d, and it shows a strong fluorescent signal. Biotinylated atto 550 on mica without GO·streptavidin gave no signal (Figure 4e), indicating that the atto 550 does not interact with the mica under these conditions. When we incubated the GO·streptavidin with non-biotinylated atto 550, there was a very-faint signal (Figure 4f), which may be attributed to a non-specific interaction of the atto 550 with the skeleton of the GO via π–π interactions. It has been reported that graphene/carbon nanotubes (CNTs) can interact with aromatic organic molecules;[37] the charge/energy transfer from the fluorophores to the graphene/CNTs through these interactions results in fluorescence quenching and low quantum yields.[38] Therefore, the strong, specific signal in Figure 4d most likely reflects the specific biotin-streptavidin interaction, rather than π–π bonding, as illustrated in the SWCNT·streptavidin complex.[29]

Biotinylated Au nanoparticles (NPs) having an average diameter of ~5 nm show a high contrast in electron microscopy. Therefore, these NPs were used to mimic biotinylated protein complexes to test the capturing capability of GO·streptavidin, as they are easily observed in TEM. The location of the biotinylated Au NPs on graphene can also help us to understand the structure of the GO·streptavidin complexes. GO·streptavidin complexes were deposited on a continuous carbon grid (O_2-plasma-treated), as shown in **Figure 5a–b**. The biotinylated Au NPs show a high contrast in TEM, and were deposited on a polylysine-treated continuous carbon grid, as shown in Figure 5c. Then we prepared GO·Au NPs conjugates on a continuous carbon grid using similar methods as used for the GO·DNA conjugates and the TEM results are shown in

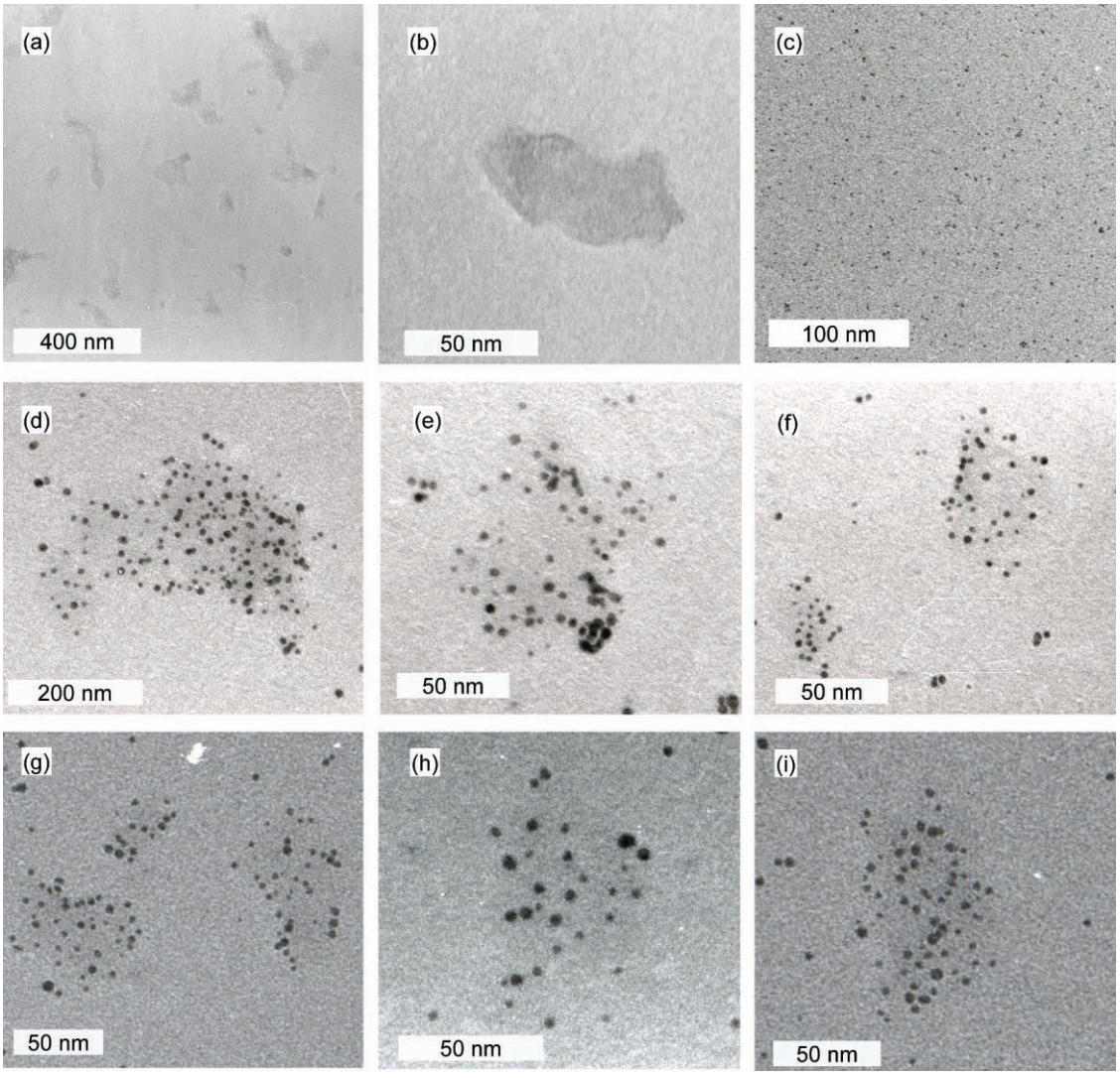

Figure 5. a–b) TEM images of the GO·streptavidin complex. c) TEM image of the biotinylated Au NPs. d–i) TEM images of the GO·Au NP conjugates prepared via the biotin-streptavidin affinity interaction using the GO·streptavidin complexes as the docking matrix.

Figure 5d–i. The results indicate a high loading of Au NPs on the GO·streptavidin complexes (especially Figure 5d and 5i), suggesting a good biotin-binding capacity. The Au NPs associated with the GO sheets had a much-higher density than the ones non-specifically adsorbed on the amorphous carbon support, indicating that the GO·streptavidin complexes can be used to specifically capture biotinylated protein complexes. The Au NPs existed as single particles on the GO, suggesting that it is also feasible for the protein complexes to be captured by GO, which can then be used for single-particle analysis.

According to the reaction scheme in Figure 2, the location of the Au NPs on GO can give us direct information about the distribution (at least partially) of streptavidin on GO. The structure of GO has been a hot topic since its discovery and its exact structure remained unclear up till now.[22c] According to the models developed so far,[22] the following oxygen functionalities exist on GO: epoxide (–O–), hydroxyl (–OH), carbonyl (–C=O), carboxyl (–COOH), and other carbonyl-containing groups (ketones/quinones). Epoxide and hydroxyl groups are the major components and locate on the basal plane of the GO; the –COOH groups locate at the edges of the GO sheets and only account for a very-low content of all of the oxygen functionalities.[39] Our observations (Figure 5d–i) indicate that the Au NPs were located not only at the edges, but also in the plane of the GO (although the edges were important locations – see especially the right side of the image in Figure 5g). This is consistent with the AFM observations in Figure 3d–e, where the streptavidin molecules were not only observed at the edges of the GO, but also in the central regions. One possible interpretation is that –COOH groups may exist both on the edges and in the plane of the GO, although further investigation is required to provide conclusive proof, as well as to address the mechanism of the introduction of the –COOH groups. The possible mechanism may be similar to the allotrope of GO–carbon nanotubes:[40] the –COOH groups may be introduced both to defective in-plane sites and at the edges of the graphene during the oxidation. Another possibility is that, besides the carbodiimide crosslinking between the $–NH_2$ groups of the biotin-PEG_8-NH_2 with the –COOH groups in GO, there may also be a ring-opening reaction of the epoxy groups, resulting from attack by the nucleophilic $–NH_2$ groups,[41] which were used to form the crosslinked colloid of GO and poly(allylamine).[42]

3. Conclusions

We have devised a novel method for preparing GO·streptavidin complexes via the biotin-streptavidin interaction. These GO·streptavidin complexes can be used for affinity purification of biotinylated protein complexes. The streptavidin is specifically tethered to the GO and the GO·streptavidin complex shows unique features such as very-high loading of streptavidin and stochastic coverage across the surface of the GO·streptavidin complex. Capturing biotinylated DNA, Au NPs, and fluorophores shows that the GO·streptavidin complexes have a very-high biotin-binding capability, thus providing a versatile affinity scaffold. The captured biotinylated Au NPs were located not only at the edges, but also in the plane of the GO, suggesting that the streptavidin tetramer also existed both at the edges and in the plane of the GO. Compared to other affinity scaffolds, GO·streptavidin complexes have the following advantages: they have a 2D planar structure and are very thin; therefore, they are electron transparent and can be used for TEM studies such as single-particle analysis; the GO·streptavidin together with the captured protein complexes can be separated from other soluble components via a filtration process or even via on-grid separation, which can be as quick as a few seconds and allows immediate EM observation, promoting maintenance of their native structure. GO·streptavidin complexes can enter living cells,[43] and may be used for in-cell purification; furthermore, they are easily made and relatively cheap, allowing bulk-quantity preparations.

4. Experimental Section

Materials: Graphite (1 mm, 99.95% purity) was purchased from Qingdao Tianhe Graphite Company. Streptavidin was purchased from ProSpec-Tany. (7-Azabenzotriazol-1-yloxy)tripyrrolidinophosphonium hexafluorophosphate (PyAOP) (96%), *N*,*N*-di-isopropylethylamine (DIEA) (99.5%, biotech. grade), *O*-(2-Aminoethyl)-*O′*-[2-(biotinylamino) ethyl]octaethylene glycol (biotin-PEG_8-NH_2) (≥95% oligomer purity, the number 8 means that the $–CH_2CH_2O–$ unit is repeated 8 times), atto 550, biotinylated atto 550, polylysine (0.1% w/v) and APTES (98%) were purchased from Sigma–Aldrich. DMF (99.8%) was purchased from Biosolve. Biotinylated Au NPs (average diameter of 5 nm, 0.01% based on Au) were purchased from NanoCS.

Preparation of the GO·Streptavidin Complex: Graphene oxide was prepared by a modification of Hummers' method[20] from flake graphite. GO (1.5 mg) was dispersed in DMF (1.5 mL, dried with a molecule sieve (4 Å) overnight), then biotin-PEG_8-NH_2 (50 mg, 0.073 mmol), PyAOP (38 mg, 0.073 mmol), and DIEA (18.9 mg, 0.146 mmol) were added. The mixture was stirred for 1 h, and then membrane-filtered (nylon, 0.22 mm, Tianjin Autoscience instrument), washed thoroughly with DMF and transferred to MilliQ H_2O. Below, the product is referred to as biotinylated GO.

The biotinylated GO solution in MilliQ water (0.01 mg mL^{-1}, for GO assay, 10 mL) was added dropwise, whilst shaking, to a streptavidin solution (1 mg mL^{-1}, 10 mL/20 mL) in phosphate buffered saline (PBS) (pH = 7.2) and then mixed for 60 min at 40 rpm using a roller mixer (Stuart, model STR9D). The mixture was washed 3 times using a centrifugation filter (Amicon Ultra-15, 100K), and dispersed in MilliQ H_2O (2 mL). The product was marked as GO·streptavidin. A Bradford assay[44] was used to determine the loading of streptavidin on GO (see Figure S3 in the SI and Table S1 for details).

Preparation of DNA, GO·DNA, GO·Atto 550, GO·Au NP Conjugates: Biotinylated and non-biotinylated 1000-bps DNA were obtained by a polymerase chain reaction (PCR), as described elsewhere.[29] GO·streptavidin (0.01 mg mL^{-1} for GO assay) was deposited on freshly cleaved mica for 10 min, then rinsed several times with water and dried gently under a stream of nitrogen gas. Solutions of biotinylated DNA (20 mg mL^{-1}, 25 mL) and biotinylated atto 550 (0.01 mg mL^{-1}, 25 mL) were placed on the GO·streptavidin-coated mica for 30 min at room temperature for the preparation of the GO·DNA and GO·atto-550 conjugates. After incubation, the mica was rinsed several times with water and dried gently under a stream of nitrogen gas. The preparation of the GO·Au-NP conjugates on continuous carbon grids (SPI, 200 mesh) was similar to the above procedure, except that the drying under a stream of nitrogen was omitted.

Measurements (AFM, FTIR Spectroscopy, Fluorescence Microscopy, UV-vis Spectroscopy, TGA, and TEM): Tapping mode at 300 Hz was used to acquire the AFM images under ambient conditions (AFM: Digital Instruments Dimension 3100). Samples of the GO·streptavidin complex and the GO·DNA conjugates were prepared as described above. FTIR-spectroscopy measurements were performed at ambient conditions

using a Perkin–Elmer FTIR spectrometer (Paragon 1000). Samples for FTIR spectroscopy were prepared with KBr to form transparent pellets. Confocal microscopy (Olympus BX51TF) was used to collect fluorescent images of the GO·atto-550 samples after excitation at 488 nm using an argon laser. UV-vis spectrophotometry (Varian Cary 50 series) was used to obtain the spectra of GO and streptavidin. UV-vis spectrophotometry (Ultrospec 110 Pro) was also used to obtain the absorbance values of GO, biotinylated GO and the GO·streptavidin complex at 320 nm, required for measuring the concentration of GO: the experimental details are shown in Figure S2 in the SI. TGA was performed on a TA Instruments TGA Q500 V6.7 Build 203 with a heating rate of 5 °C min^{-1} in N_2 flow. TEM images were obtained using a JEOL JEM-1010 electron microscope, with an acceleration voltage of 80 kV.

Supporting Information

Supporting Information is available online from Wiley InterScience or from the author.

Acknowledgements

The authors gratefully acknowledge financial support from the Cyttron Foundation (http://www.cyttron.org) and the Netherlands Organisation for Scientific Research (NWO) Veni grant 2009 (Project Number: 700.59.407). We thank Hermen Overkleeft, Dmitri Filippov, Richard van den Berg, Nan Li, Patrick Voskamp, Donglin Tang and G.A. van Albada for technical support.

Received: April 21, 2010
Published online: July 13, 2010

[1] E. M. Phizicky, S. Fields, *Microbiol. Rev.* **1995**, *59*, 94.
[2] a) A. Ullrich, J. Schlessinger, *Cell* **1990**, *61*, 203; b) M. J. Berridge, R. F. Irvine, *Nature* **1984**, *312*, 315.
[3] C. E. Samuel, *Clin. Microbiol. Rev.* **2001**, *14*, 778.
[4] L. Giot, J. S. Bader, C. Brouwer, A. Chaudhuri, B. Kuang, Y. Li, Y. L. Hao, C. E. Ooi, B. Godwin, E. Vitols, G. Vijayadamodar, P. Pochart, H. Machineni, M. Welsh, Y. Kong, B. Zerhusen, R. Malcolm, Z. Varrone, A. Collis, M. Minto, S. Burgess, L. McDaniel, E. Stimpson, F. Spriggs, J. Williams, K. Neurath, N. Ioime, M. Agee, E. Voss, K. Furtak, R. Renzulli, N. Aanensen, S. Carrolla, E. Bickelhaupt, Y. Lazovatsky, A. DaSilva, J. Zhong, C. A. Stanyon, R. L. Finley, K. P. White, M. Braverman, T. Jarvie, S. Gold, M. Leach, J. Knight, R. A. Shimkets, M. P. McKenna, J. Chant, J. M. Rothberg, *Science* **2003**, *302*, 1727.
[5] a) R. Henderson, *Q. Rev. Biophysics* **2004**, *37*, 3; b) T. Berggard, S. Linse, P. James, *Proteomics* **2007**, *7*, 2833.
[6] S. Fields, O. K. Song, *Nature* **1989**, *340*, 245.
[7] a) R. Karlsson, A. Michaelsson, L. Mattsson, *J. Immunological Methods* **1991**, *145*, 229; b) U. Jonsson, L. Fagerstam, B. Ivarsson, B. Johnsson, R. Karlsson, K. Lundh, S. Lofas, B. Persson, H. Roos, I. Ronnberg, S. Sjolander, E. Stenberg, R. Stahlberg, C. Urbaniczky, H. Ostlin, M. Malmqvist, *BioTechniques* **1991**, *11*, 620.
[8] K. Asai, Y. Ueno, C. Sato, K. Takahashi, *Genome Informatics Ser. Workshop Genome Informatics* **2000**, *11*, 151.
[9] a) O. Puig, F. Caspary, G. Rigaut, B. Rutz, E. Bouveret, E. Bragado-Nilsson, M. Wilm, B. Seraphin, *Methods* **2001**, *24*, 218; b) T. Burckstummer, K. L. Bennett, A. Preradovic, G. Schutze, O. Hantschel, G. Superti-Furga, A. Bauch, *Nat. Methods* **2006**, *3*, 1013.
[10] a) F. E. Regnier, *J. Chromatogr. B: Biomedical Sci Appl.* **1987**, *418*, 115; b) R. J. Austin, M. D. Biggin, *Proc. Natl. Acad. Sci. USA* **1996**, *93*, 5788.
[11] a) J. Sperling, R. Sperling, *Nucleic Acids Res.* **1978**, *5*, 2755; b) J. Toth, M. D. Biggin, *Nucleic Acids Res.* **2000**, *28*, e4.
[12] H. Strutt, G. Cavalli, R. Paro, *EMBO J.* **1997**, *16*, 3621.
[13] C. M. Niemeyer, *Angew. Chem. Int. Ed.* **2001**, *40*, 4128.
[14] A. A. Balandin, S. Ghosh, W. Z. Bao, I. Calizo, D. Teweldebrhan, F. Miao, C. N. Lau, *Nano Lett.* **2008**, *8*, 902.
[15] S. Stankovich, D. A. Dikin, G. H. B. Dommett, K. M. Kohlhaas, E. J. Zimney, E. A. Stach, R. D. Piner, S. T. Nguyen, R. S. Ruoff, *Nature* **2006**, *442*, 282.
[16] a) K. S. Novoselov, A. K. Geim, S. V. Morozov, D. Jiang, M. I. Katsnelson, I. V. Grigorieva, S. V. Dubonos, A. A. Firsov, *Nature* **2005**, *438*, 197; b) A. K. Geim, K. S. Novoselov, *Nat. Mater.* **2007**, *6*, 183; c) A. H. Castro Neto, F. Guinea, N. M. R. Peres, K. S. Novoselov, A. K. Geim, *Rev. Mod. Phys.* **2009**, *81*, 109; d) Y. B. Zhang, Y. W. Tan, H. L. Stormer, P. Kim, *Nature* **2005**, *438*, 201.
[17] C. T. Nottbohm, A. Beyer, A. S. Sologubenko, I. Ennen, A. Hutten, H. Rosner, W. Eck, J. Mayer, A. Golzhauser, *Ultramicroscopy* **2008**, *108*, 885.
[18] a) T. J. Booth, P. Blake, R. R. Nair, D. Jiang, E. W. Hill, U. Bangert, A. Bleloch, M. Gass, K. S. Novoselov, M. I. Katsnelson, A. K. Geim, *Nano Lett.* **2008**, *8*, 2442; b) J. C. Meyer, C. O. Girit, M. F. Crommie, A. Zettl, *Nature* **2008**, *454*, 319.
[19] a) N. R. Wilson, P. A. Pandey, R. Beanland, R. J. Young, I. A. Kinloch, L. Gong, Z. Liu, K. Suenaga, J. P. Rourke, S. J. York, J. Sloan, *ACS Nano* **2009**, *3*, 2547; b) R. S. Pantelic, J. C. Meyer, U. Kaiser, W. Baumeister, J. r. M. Plitzko, *J. Struct. Biol.* **2010**, *170*, 152.
[20] a) W. S. Hummers, R. E. Offeman, *J. Am. Chem. Soc.* **2002**, *80*, 1339; b) M. Hirata, T. Gotou, S. Horiuchi, M. Fujiwara, M. Ohba, *Carbon* **2004**, *42*, 2929.
[21] a) A. Chapman-Smith, J. E. Cronan, *Biomolecular Eng.* **1999**, *16*, 119; b) E. de Boer, P. Rodriguez, E. Bonte, J. Krijgsveld, E. Katsantoni, A. Heck, F. Grosveld, J. Strouboulis, *Proc. Natl. Acad. Sci. USA* **2003**, *100*, 7480.
[22] a) A. Lerf, H. Y. He, M. Forster, J. Klinowski, *J. Phys. Chem. B* **1998**, *102*, 4477; b) T. Szabo, O. Berkesi, P. Forgo, K. Josepovits, Y. Sanakis, D. Petridis, I. Dekany, *Chem. Mater.* **2006**, *18*, 2740; c) D. R. Dreyer, S. Park, C. W. Bielawski, R. S. Ruoff, *Chem. Soc. Rev.* **2010**, *39*, 228.
[23] J. I. Paredes, S. Villar-Rodil, A. Martinez-Alonso, J. M. D. Tascon, *Langmuir* **2008**, *24*, 10560.
[24] S. Park, K. S. Lee, G. Bozoklu, W. Cai, S. T. Nguyen, R. S. Ruoff, *ACS Nano* **2008**, *2*, 572.
[25] a) H. Y. He, T. Riedl, A. Lerf, J. Klinowski, *J. Phys. Chem.* **1996**, *100*, 19954; b) H. Y. He, J. Klinowski, M. Forster, A. Lerf, *Chem. Phys. Lett.* **1998**, *287*, 53; b) A. Lerf, H. Y. He, T. Riedl, M. Forster, J. Klinowski, *Solid State Ionics* **1997**, *101*, 857.
[26] T. Szabo, O. Berkesi, I. Dekany, *Carbon* **2005**, *43*, 3186.
[27] M. J. Fernández-Merino, L. Guardia, J. I. Paredes, S. Villar-Rodil, P. Solís-Fernández, A. Martínez-Alonso, J. M. D. Tascón, *J. Phys. Chem. C* **2010**, *114*, 6426.
[28] M. Wilchek, E. A. Bayer, *Anal. Biochem.* **1988**, *171*, 1.
[29] Z. Liu, F. Galli, K. G. H. Janssen, L. Jiang, H. J. Van Der Linden, D. C. de Geus, P. Voskamp, M. E. Kuil, R. C. L. Olsthoorn, T. H. Oosterkamp, T. Hankemeier, J. P. Abrahams, *J. Phys. Chem. C* **2010**, *114*, 4345.
[30] a) S. Connolly, D. Fitzmaurice, *Adv. Mater.* **1999**, *11*, 1202; b) S. Cobbe, S. Connolly, D. Ryan, L. Nagle, R. Eritja, D. Fitzmaurice, *J. Phys. Chem. B* **2003**, *107*, 470.
[31] a) F. X. Li, Z. F. Lu, H. T. Qian, J. M. Rui, S. N. Chen, P. Jiang, Y. L. An, H. F. Mi, *Macromolecules* **2004**, *37*, 764; b) F. X. Li, Z. F. Liu, X. P. Liu, X. Y. Yang, S. N. Chen, Y. L. An, J. Zuo, B. L. He, *Macromolecules* **2005**, *38*, 69.
[32] X. Z. Zhou, X. Huang, X. Y. Qi, S. X. Wu, C. Xue, F. Y. C. Boey, Q. Y. Yan, P. Chen, H. Zhang, *J. Phys. Chem. C* **2009**, *113*, 10842.

[33] J. Kong, H. J. Dai, *J. Phys. Chem. B: Condens. Matter* **2001**, *105*, 2890.
[34] O. Leenaerts, B. Partoens, F. M. Peeters, *Phys. Rev. B: Condens. Matter* **2008**, *77*, 125416.
[35] a) D. M. Czajkowsky, Z. Shao, *J. Microsc.* **2003**, *211*, 1; b) A. Ebner, L. Wildling, R. Zhu, C. Rankl, T. Haselgrubler, P. Hinterdorfer, H. J. Gruber, in *Topics in Current Chemistry*, Vol. *285*, Springer, Berlin **2008**, p. 29.
[36] S. Niyogi, E. Bekyarova, M. E. Itkis, J. L. McWilliams, M. A. Hamon, R. C. Haddon, *J. Am. Chem. Soc.* **2006**, *128*, 7720.
[37] Y. Tomonari, H. Murakami, N. Nakashima, *Chem. Eur. J.* **2006**, *12*, 4027.
[38] a) M. Bottini, F. Cerignoli, M. I. Dawson, A. Magrini, N. Rosato, T. Mustelin, *Biomacromolecules* **2006**, *7*, 2259; b) Q. Liu, Z. F. Liu, X. Y. Zhong, L. Y. Yang, N. Zhang, G. L. Pan, S. G. Yin, Y. Chen, J. Wei, *Adv. Funct. Mater.* **2009**, *19*, 894; c) Z. F. Liu, Q. Liu, Y. Huang, Y. F. Ma, S. G. Yin, X. Y. Zhang, W. Sun, Y. S. Chen, *Adv. Mater.* **2008**, *20*, 3924.
[39] X. F. Gao, J. Jang, S. Nagase, *J. Phys. Chem. C* **2010**, *114*, 832.
[40] a) D. Tasis, N. Tagmatarchis, A. Bianco, M. Prato, *Chem. Rev.* **2006**, *106*, 1105; b) J. Liu, A. G. Rinzler, H. Dai, J. H. Hafner, R. K. Bradley, P. J. Boul, A. Lu, T. Iverson, K. Shelimov, C. B. Huffman, F. Rodriguez-Macias, Y. S. Shon, T. R. Lee, D. T. Colbertx, R. E. Smalley, *Science* **1998**, *280*, 1253.
[41] R. T. Morrison, R. N. Boyd, *Organic Chemistry*, 2nd ed., Prentice Hall, Inc., New Jersey **1992**.
[42] S. Park, D. A. Dikin, S. T. Nguyen, R. S. Ruoff, *J. Phys. Chem. C* **2009**, *113*, 15801.
[43] X. M. Sun, Z. Liu, K. Welsher, J. T. Robinson, A. Goodwin, S. Zaric, H. J. Dai, *Nano Res.* **2008**, *1*, 203.
[44] M. M. Bradford, *Anal. Biochem.* **1976**, *72*, 248.